

# IN-VIVO MEASUREMENT OF TIBIOTALAR JOINT MOTION: ACCURACY ASSESSMENT AND PRELIMINARY RESULTS

Sukhinder K. Bilkhu<sup>1</sup>, Stephanie K. Kline<sup>1</sup>, Mitch J. Mager<sup>1</sup>, Jason J. Davis<sup>2</sup>, Richard L. Needleman<sup>2</sup>, Michael J. Bey<sup>1</sup>

<sup>1</sup>Bone & Joint Center, <sup>2</sup>Department of Orthopaedic Surgery, Henry Ford Hospital, 2799 W. Grand Blvd, Detroit, MI 48202, USA, [sbilkhu1@hfhs.org](mailto:sbilkhu1@hfhs.org)

## INTRODUCTION

Adult acquired flatfoot deformity (AAFD) is a chronic debilitating foot and ankle condition that is very common. It is often caused by posterior tibial tendon dysfunction, where the tendon no longer supports the navicular, causing a collapsed arch. AAFD is believed to cause a shift in tibiotalar joint contact patterns and eventually lead to arthritis. The ability to accurately measure foot and ankle motion and, in particular, tibiotalar joint contact patterns is critical to understanding the etiology and treatment of AAFD. The objectives of this study were to: 1) assess the accuracy of a model-based tracking technique for measuring in-vivo foot and ankle motion and 2) demonstrate the application of this technique by quantifying tibiotalar joint contact patterns.

## METHODS AND PROCEDURES

*In-Vitro Accuracy Assessment:* To assess the accuracy of our technique for measuring in-vivo foot and ankle motion, a matched pair of fresh-frozen cadaveric lower legs was thawed to room temperature. Under fluoroscopic guidance, three 1.6 mm diameter tantalum beads were inserted in both the tibia and talus. Biplane x-ray images were acquired as the specimen was manually moved to simulate plantarflexion, dorsiflexion and tibial rotation. Each trial was 2 seconds in duration, the biplane x-ray images were collected at 120 Hz, and 18 total trials were collected (2 specimens, 3 trials per motion). Following

testing, CT images of the entire foot and ankle complex were acquired. The talus and tibia were manually segmented from surrounding tissues and reconstructed into 3D specimen-specific bone models.

The positions of the tibia and talus were tracked from the biplane x-ray images using a previously described model-based tracking technique (Bey 2006). Briefly, this method tracks the 3D position and orientation of each bone based on its 3D shape and density. For comparison, the position of each bone was also determined from the biplane x-ray images by tracking the implanted tantalum beads with an accurate ( $\pm 0.1$  mm) dynamic radiostereometric analysis (RSA) technique (Tashman 2003). These RSA data were used as the “gold standard” for this comparison. Accuracy of the model-based tracking technique was measured by comparing the 3D bead positions determined with model-based tracking to the 3D bead positions determined with dynamic RSA. Specifically, accuracy was quantified by calculating the RMS error between the two measurement techniques.

*In-Vivo Human Testing:* To demonstrate the utility of this measurement technique, we then tracked the position and orientation of the tibia and talus during gait from two male subjects. The subjects included one with no history of foot or ankle injury (i.e., a normal subject) and one with a clinical diagnosis of AAFD. The normal subject was tested once and the AAFD subject was tested twice: once with an arch-support orthotic in his shoe and

once without the orthotic. Each subject walked at a comfortable speed with their right foot centered in the biplane x-ray system's imaging field during the stance phase of the gait cycle. Following testing, CT scans of the entire foot/ankle complex were acquired for both subjects. 3D bone models of the tibia and talus were reconstructed from the CT images. The positions of the tibia and talus were then determined from the biplane x-ray images using model-based tracking.

Tibiotalar joint contact patterns were determined using a previously reported technique that combines the joint motion measured from the biplane x-ray images with the CT-based bone models (Anderst 2003). Specifically, this technique calculated the distance between the articulating surfaces of the tibia and talus at each frame of data. Tibiotalar joint contact was defined as occurring in those regions where the tibiotalar joint space was  $\leq 2$  mm. After defining an anatomical coordinate system for the talus with an axis bisecting the talar dome into medial and lateral aspects, we calculated a distance-weighted distribution of medial/lateral joint contact.

## RESULTS

There was excellent agreement between the model-based tracking and dynamic RSA techniques. Specifically, the RMS error between the two measurement techniques was  $\pm 0.7$  mm for both the tibia and talus.

The joint contact patterns demonstrated that the normal subject had a higher percentage of contact on the medial portion of the talar dome. In contrast, the AAFD subject experienced a more even distribution of contact between medial and lateral portions of the talar dome. This distribution of contact shifted slightly more medially with the addition of the orthotic (Figure 1, Table 1).

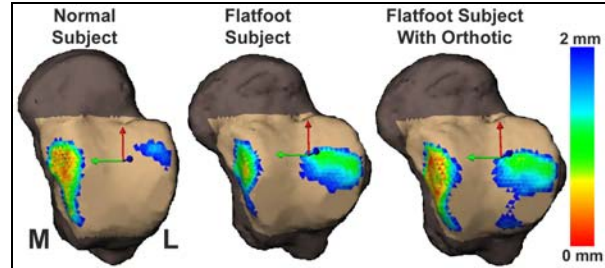


**Figure 1.** Tibiotalar joint contact patterns during the midstance phase of gait for a normal subject, flatfoot subject, and flatfoot subject with an orthotic. M=medial, L=lateral.

Condition	Medial	Lateral
Normal	83.2%	16.8%
Flat Foot	49.8%	50.2%
Flat Foot w/Orthotic	54.1%	45.9%

**Table 1.** Contact distribution between medial and lateral portions of the tibiotalar joint.

## DISCUSSION

This study assessed the accuracy and demonstrated the utility of a technique for measuring in-vivo tibiotalar joint motion. The study indicated that the model-based tracking technique can measure the motion of the tibia and talus to an accuracy of within  $\pm 0.7$  mm. An analysis of the tibiotalar joint contact patterns suggests that this technique is sensitive to identifying subtle differences in joint mechanics between subjects. Future research will use this experimental approach to characterize joint contact patterns at the tibiotalar, talonavicular and subtalar joints. These data will be used to assess the etiology and treatment of AAFD and to improve upon the design of total ankle joint replacements.

## REFERENCES

- Anderst, W. J. and S. Tashman (2003). *Journal of Biomechanics* 36: 1291-1299.
- Bey, M.J., R. Zauel, et al. (2006). *J Biomech Eng* 128(4): 604-9.
- Tashman, S. and W. Anderst (2003). *J Biomech Eng* 125(2): 238-45.